Journal of
Engineering, Computing and Architecture ISSN 1934-7197
Volume 2, Issue 1, 2008

Effectiveness of Energy Dissipaters Type Friction on the Reduction of the Inelastic Seismic Responses of Moment Steel Frames

Alfredo Reyes-Salazar, Professor, Universidad Autónoma de Sinaloa, **reyes@uas.uasnet.mx**
Juan de Dios Garay-Morán, Graduate Student, **juandediosgaray@hotmail.com**
Arturo López-Barraza, Assistant Professor, Universidad Autónoma de Sinaloa, **alópezb@uas.uasnet.mx**

Abstract

The effectiveness of energy dissipaters type friction on the reduction of the inelastic seismic responses of moment steel frames (MSF) is studied. The energy dissipater devices (EDD) are placed in the beam-column joints. The parameters of the dissipaters are modified to vary the magnitude of the friction force. The results of the study indicate that EDD based on friction of metals can significantly reduce the seismic response of MSF. The magnitude of the reduction, in terms of interstory displacements, decreases with the fundamental period of the models used, but the reduction for interstory shears is similar for all the models. Results also indicate that many plastic hinges are formed in the frame without energy dissipaters, but no plastic hinges are developed, in general, in the frames with energy dissipaters. It indicates that using energy dissipaters type friction protect the frames from significantly yielding. It is shown that the equivalent viscous damping of energy dissipaters type friction can be much larger than that existing in a bare steel frame ($\xi \approx 2\%$). Based on these findings, design response spectra for MSF with energy dissipaters type friction can be developed for specific sites by using appropriate amounts of equivalent viscous damping.

Introduction

Among the different structural configurations used for steel frames in regions of high seismicity, moment steel frames (MSF) have been the most popular. Architects and owners prefer to use this system because of lack of bracing, which provides maximum flexibility for space utilization. Even though, the member sizes of MSF are normally increased to meet the building code's drift requirements, it is customarily considered a good exchange for bracing elements. In addition, MSF are popular because they are considered as highly ductile systems. Code-specified seismic procedures typically assign the largest force reduction factor (*R*) to MSF, implying the largest ductility and the lowest lateral design forces. However, recent earthquakes in the United States (Northridge 1994) and Japan (Kobe 1995) have demonstrated that the seismic behavior of MRSF was not as expected. Several frames, many of them recently constructed, suffered failure in their connections. It is generally accepted that the seismic behavior of buildings strongly depends on their energy dissipation capacity. In a MSF the major sources of energy dissipation are due to viscous damping (E_D) and the hysteretic behavior of the material (E_P) at the location of plastic hinges. Plastic energy however, is accompanied by significant nonlinear response, which constitutes substantial damage to the seismic framing system. If one part of the input energy is dissipated through special devices, which can be easily replaced after the occurrence of a severe earthquake, the structural damage caused by yielding of the material will be reduced. The use of energy dissipating devices is a promising approach to the problem.

Literature review

Several energy dissipater devices have been developed and tested around the world. It has been shown that these devices increase the energy dissipation capacity of buildings without significantly changing their natural periods. They can be used in new structures or in existing ones, which don't have enough resistance to seismic loading. Devices within a structure used to dissipate energy introduced by an earthquake are referred as Passive Energy Dissipaters. According to their behavior, Passive Energy Dissipaters are classified (ATC 1995) as hysteretic and velocity-dependent. Hysteretic dampers in turn include those based on friction and yielding of metals. Examples of velocity-dependant dampers include those consisting of viscoelastic solid materials or fluids and those operating by forcing fluids through an orifice. It has been shown (Pong et al 1994), that the maximum base shear and displacements of a structure can be significantly reduced when passive dampers of the second group are used. However, it is also recognized that the construction of some of these devices is not economical and consequently their use is not generalized yet.

Energy dissipaters based on friction of metals have been tested by researchers (Pall and Marsh 1987, Aiken and Kelly 1990). They represent a good alternative for several reasons: a) it has been shown that the hysteretic cycles of these devices are nearly elasto-plastic, b) they don't present stiffness degradation during several dozen of cycles (Pall 1989, Grigorian et al 1993), c) they are easy to construct, and d) the magnitude of their yielding force can be economically modified by varying the thickness of the component plates and the normal force. One of the energy dissipaters based on friction of metal broadly tested is that proposed by Pall (1989). The system basically consists of an inexpensive mechanisms containing friction brake lining pads placed at the intersection of the frame cross-braces. The performance of this model was analytically and experimentally tested by Filiatrault and Cherry (1997) by using a 1/3 scale three-story one-bay frame. The results clearly showed the superior performance of the frame with energy dissipaters compared to conventional building systems. The Pall Model was also experimentally studied by Kullman and Cherry (1996) by using a full-scale one-story one-bay frame. The results of the test indicated that the friction damper provides a nearly rectangular and repeatable hysteresis curve. Kullman and Cherry also performed an analytical study by using a six-story frame with and without dissipaters. Comparisons between the response of the friction damped frame and the conventional braced frame indicate that, for the frame model under consideration, the response in terms of moments and interstory displacements was not necessarily improved in all stories when energy dissipaters were used. However, the friction dampers protect all the main structural elements from yielding.

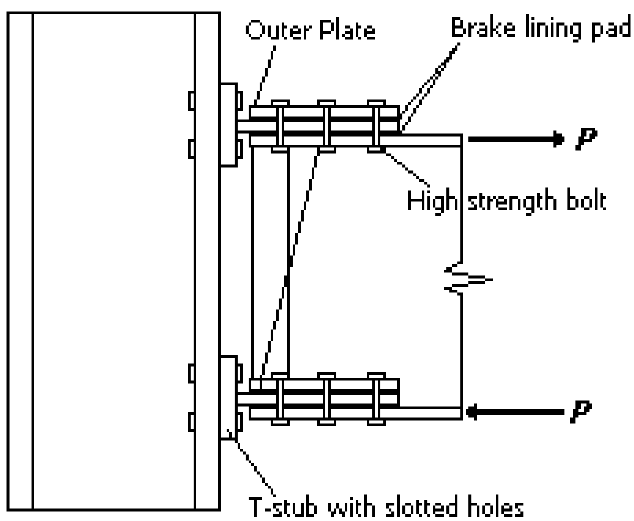

Fig. 1. Zhao and Ha´s Model

Another energy dissipater based on friction of metals was proposed by Grigorian et al (1993). This device consists of slotted bolted connections, which are designed to dissipate energy through friction during rectilinear tension and compression loading cycles. The development of this device requires only slight modification of standard construction practice and requires materials, which are widely available commercially. The performance of this dissipater was analytical and experimentally tested by Grigorian by using a one-story one-bay diagonally braced frame under the action of several earthquakes. The results of the study indicated that, on the average, close to 85% of the total input energy is dissipated by the dissipater. However, as the dissipater proposed by Pall, braced elements are required to place the device.

Recently, Zhao and Ha (1996) proposed an energy dissipater type friction. This device is similar to that proposed by Grigorian. However, the dissipater is located at the beam-column connection. The device basically consists of two-slotted T-stub, which connects beam and columns as shown in Fig. 1. High strength bolts are inserted in the slotted holes. The T-stub may be replaced with angles or welded plates. The friction connection also includes an outer plate and brake lining pads placed as shown in Fig. 1. The bolts press the two brake lining pads against the faces of the T-stub. As the T-stubs move within the slotted holes, frictional forces develop producing energy dissipation. The friction joints are designed not to slip under service load, but are expected to slip under a severe earthquake. One of the advantages of this energy dissipation device is that no braced elements are required to place the dissipater. The performance of this dissipater was analytically tested by Zhao and Ha by using two steel frames having 8 and 20 stories under the action of four strong motions. The numerically study indicates that the interstory displacements and base shear can be significantly reduced when the above-mentioned connection is used.

Objectives of the study

The effectiveness of energy dissipaters type friction on the reduction of the inelastic seismic responses of MSF is addressed in this paper. The dissipaters are placed in the beam-column joints. Several MSF, representative of the short, medium and long period ranges, and several strong motions, representative of medium and stiff local soil conditions, are used in the study. The parameters of the dissipater are modified to vary the magnitude of the force friction. Their efficiency in terms of equivalent viscous damping is evaluated. The authors and their associates developed a finite element-based algorithm in the time domain which is used to evaluate the nonlinear seismic response of steel frames. The algorithm is able to model energy dissipaters and is used in the study. This is elaborated further below.

Mathematical formulation

To satisfy the objectives of the study, the seismic responses of steel frame models are evaluated as accurately as possible by using an assumed stress-based finite element algorithm developed by the authors and their associates (Gao and Haldar 1995, Reyes-Salazar, 1997). The procedure estimates nonlinear seismic responses in time domain considering all major sources of nonlinearity. Material and geometric nonlinearity and that nonlinearity introduced by the dissipaters can be considered. In this approach, an explicit form of the tangent stiffness matrix is derived without any numerical integration. Fewer elements can be used in describing a large deformation configuration without sacrificing any accuracy, and the material and dissipater nonlinearity can be incorporated without losing its basic simplicity (Kondo and Atluri 1987). It gives very accurate results and is very efficient compared to the commonly used displacement-based approaches. The procedure and the algorithm have been extensively verified using available theoretical and experimental results (Reyes-Salazar and Haldar 2001, Haldar and Nee 1989). Only the basic equations are presented here for the ready reference purpose. The linear iterative strategy is used to solve the nonlinear dynamic equation of motion as:

$$\mathbf{m}\,{}^{(t+\Delta t)}\ddot{\mathbf{U}}^{(k)} + {}^{t}\mathbf{C}^{(t+\Delta t)}\,\dot{\mathbf{U}}^{(k)} + {}^{t}\mathbf{K}^{(t+\Delta t)}\,\Delta\mathbf{U}^{(k)} = {}^{(t+\Delta t)}\mathbf{F}^{(k)} - {}^{(t+\Delta t)}\mathbf{R}^{(k-1)} - \mathbf{m}\,\ddot{\mathbf{U}}_{g}^{(k)} \qquad \textbf{(1)}$$

where **m**, **C** and ${}^{t}\mathbf{K}$ are the mass, damping and the tangent stiffness matrixes, respectively. $\ddot{\mathbf{U}}$ and $\dot{\mathbf{U}}$ are the acceleration and velocity vectors, respectively, $\Delta\mathbf{U}$ is the incremental displacement vector, **F** is the external load vector, **R** is the internal force vector and $\ddot{\mathbf{U}}_{g}$ is the ground acceleration vector. Superscripts ($t + \Delta t$) and (k) indicate the time and the iteration number, respectively.

Rayleigh-type damping is commonly used for nonlinear analysis in the profession since it is a function of the mass and stiffness matrices representing the current state of a structure and is used in this study. The friction connection is represented by a partially retrained (PR) connection, which in turn is modeled by using the Richard's Model (Richard 1993). Explicit expressions for the tangent stiffness matrix and the internal force vector are developed for each beam-column element using the assumed stress-based finite element method for the kth iteration at time t. The nonlinear elastic tangent stiffness matrix for a beam-column element, $\mathbf{K}^{e}$, can be represented as:

$$\mathbf{K}^{e}=\mathbf{A}_{\sigma do}^{T}\mathbf{A}_{\sigma\sigma}^{-1}\mathbf{A}_{\sigma do}+\mathbf{A}_{ddo} \quad \textbf{(2)}$$

where $\mathbf{A}_{\sigma\sigma}^{-1}$ is the elastic property matrix, $\mathbf{A}_{\sigma do}$ is the transformation matrix and $\mathbf{A}_{ddo}$ is the geometric stiffness matrix. Similarly, the internal force vector of an element level, $\mathbf{R}^e$, can be expressed as:

$$\mathbf{R}^{e}=-\mathbf{A}_{\sigma do}^{T}\mathbf{A}_{\sigma\sigma}^{-1}\mathbf{R}_{\sigma}+\mathbf{R}_{do} \quad \textbf{(3)}$$

where $\mathbf{R}_{do}$ is the homogeneous part of the internal force vector and $\mathbf{R}_{\sigma}$ is the deformation difference vector. It is not possible to give explicit expressions for all the terms in Eqs. 2 and 3 due to lack of space, but they can be found in the literature (Reyes-Salazar and Haldar 2001, Haldar and Nee 1989).

The nonlinear structural behavior discussed above also needs to be modified to consider material nonlinearity. In this study, the material is considered to be linear elastic except at plastic hinges. Concentrated plasticity behavior is assumed at plastic hinge locations. For mathematical modeling, plastic hinges are assumed to occur at locations where the combined action of axial force, torsional and bending moments satisfies a prescribed yield function. This is discussed in detail elsewhere by Gao and Haldar (1995). The yield function for three-dimensional beam-column elements and W-type sections (used in this study) has the following form:

$$\left(\frac{P}{P_n}\right)^2+\left(\frac{M_X}{M_{nX}}\right)^2+\left(\frac{M_Y}{M_{nY}}\right)^2+\left(\frac{M_Z}{M_{nZ}}\right)^2-1=0 \quad \textbf{(4)}$$

where P is the axial force, M_x and M_y are the bending moments with respect to the mayor and minor axis, respectively, M_z is the torsional moment, P_n is the axial strength, M_{nx} and M_{ny} are the flexural strength with respect to the major and minor axis, respectively, and M_{nz} is the torsional strength. The presence of plastic hinges in the structure will produce additional axial deformation and relative rotation in a particular element. Thus, the tangent stiffness matrix needs to be modified if plastic hinges form. The elasto-plastic tangent stiffness matrix $\mathbf{K}_p$ and the elasto-plastic internal force vector $\mathbf{R}_p$ can be obtained by modifying the corresponding elastic matrixes as (Haldar and Nee 1989, Shi and Atluri 1988):

$$\mathbf{K}_{P}^{e}=\mathbf{K}^{e}-\mathbf{A}_{\sigma do}^{T}\mathbf{A}_{\sigma\sigma}^{-1}\mathbf{V}_{P}\mathbf{C}_{P}^{T}\mathbf{A}_{\sigma do} \quad \textbf{(5)}$$

$$\mathbf{R}_{P}^{e}=\mathbf{A}_{\sigma do}^{T}(\mathbf{A}_{\sigma\sigma}^{-1}\mathbf{V}_{P}\mathbf{C}_{P}^{T}-\mathbf{A}_{\sigma\sigma}^{-1})\hat{\mathbf{R}}_{\sigma}+\mathbf{R}_{do} \quad \textbf{(6)}$$

In Eqs. 5 and 6, $\mathbf{V}_{\mathbf{P}}$, $\mathbf{C}_{\mathbf{P}}$ and $\hat{\mathbf{R}}_{\sigma}$ can be shown to be:

$$\mathbf{V}_{P}=\left[\frac{-\partial f}{\partial N},\frac{-\partial f}{\partial M}\left(1-\frac{x}{l}\right),\frac{-\partial f}{\partial M}\left(\frac{x}{l}\right)\right]^{T} \quad \textbf{(7)}$$

$$\mathbf{C}_{P}^{T}=\left(\mathbf{V}_{P}^{T}\mathbf{A}_{\sigma\sigma}^{-1}\right)^{-1}\mathbf{V}_{P}^{-1}\mathbf{A}_{\sigma\sigma}^{-1} \quad \textbf{(8)}$$

$$\hat{\mathbf{R}}_{\sigma}=\mathbf{R}_{\sigma}+\begin{Bmatrix} H_P \\ \theta_P^{*}\left(1-\frac{X}{l}\right) \\ \theta_P^{*}\left(\frac{X}{l}\right)\end{Bmatrix} \quad \textbf{(9)}$$

In Eq. 9, H_p and θ_P^{*} are the additional axial elongation and additional relative rotation due to plastic hinges.

Depending on the level of earthquake excitation, all the elements in a typical structure may remain elastic, or some of the elements may remain elastic and the rest may yield. As stated earlier, the structural stiffness matrix can be explicitly obtained by considering individual elements and the corresponding element stiffness matrixes, depending on the particular state they are in. If a particular element is in an elastic state, Eqs. 2 and 3 can be used. If the element has yielded, Eqs. 5 and 6 should be used instead.

A computer program has been developed to implement the procedure. The program was extensively verified using information available in the literature. The structural response behavior in terms of members' forces, interstory base shears and interstory displacements, can be estimated using the computer program.

Dissipater modeling

In this study the dissipater will be modeled as a PR connection. A Connection is a structural element that transmits resultant stresses (axial and shear forces, torsion and bending moments) between beams and columns. Almost all steel connections used in frames are essentially PR connections with different rigidities. For plane structures, the case addressed in this paper, the torsion effect on connection deformation can be neglected. Furthermore, it has been shown that the effect of shear and axial forces is small in comparison with that of bending moment and can also be neglected (Reyes-Salazar and Haldar 2000). Thus, the bending moment at the connections and the corresponding relative rotation, generally referred as moment-relative rotation (*M-θ*) curves, are used to represent the flexible behavior of connections.

Many alternatives are available in the literature to define *M-θ* curves to represent the PR connection behavior, i.e., piecewise linear, polynomial, exponential, B-spline, and the Richard model. The Richard four-parameter model is applicable to a wide variety of connections. It was developed using experimental data. According to the model, the *M-θ* curve is given by:

$$M = \frac{(k - k_p)\theta}{\left(1 + \left|\frac{(k - k_p)\theta}{M_o}\right|^N\right)^{\frac{1}{N}}} + k_p\theta \qquad \textbf{(10)}$$

where k is the initial or elastic stiffness, k_p is the plastic stiffness, M_0 is the reference moment, and N is the curve shape parameter. The physical definition of these parameters is shown in Fig. 2.

Eq. (10) represents the monotonically increasing loading section of the connections. In a typical seismic analysis, at a given time, some of the connections are expected to be loading and others are expected to be unloading and reloading. Studies related to the unloading and reloading behavior at PR connections, both experimental and theoretical, are rare. Thus, the unloading and reloading behavior of the M-θ curves is essential. This subject has been addressed in the literature (Colson, 1991; El-Salti, 1992). In these studies, the monotonic loading behavior and the Masing rule are used to theoretically develop the unloading and reloading sections of the connections. A general class of Masing models can be defined with a virgin loading curve as:

$$f\,(M,\theta) = 0 \qquad \textbf{(11)}$$

and its unloading and reloading curve can be described by the following equation:

$$f\left(\frac{M - M_a}{2}, \frac{\theta - \theta_a}{2}\right) = 0 \qquad \textbf{(12)}$$

where (M_a, θ_a) denotes the load reversal point as shown in Fig 3.
Using the Masing rule and the Richard Model represented by Eq. (10), the mathematical model used in this study for the unloading and reloading behavior of a connection is given by:

$$M = M_a - \frac{(K - K_p)(\theta_a - \theta)}{\left(1 + \left|\frac{(K - K_p)(\theta_a - \theta)}{2M_0}\right|^N\right)^{\frac{1}{N}}} - K_p(\theta_a - \theta) \quad \textbf{(13)}$$

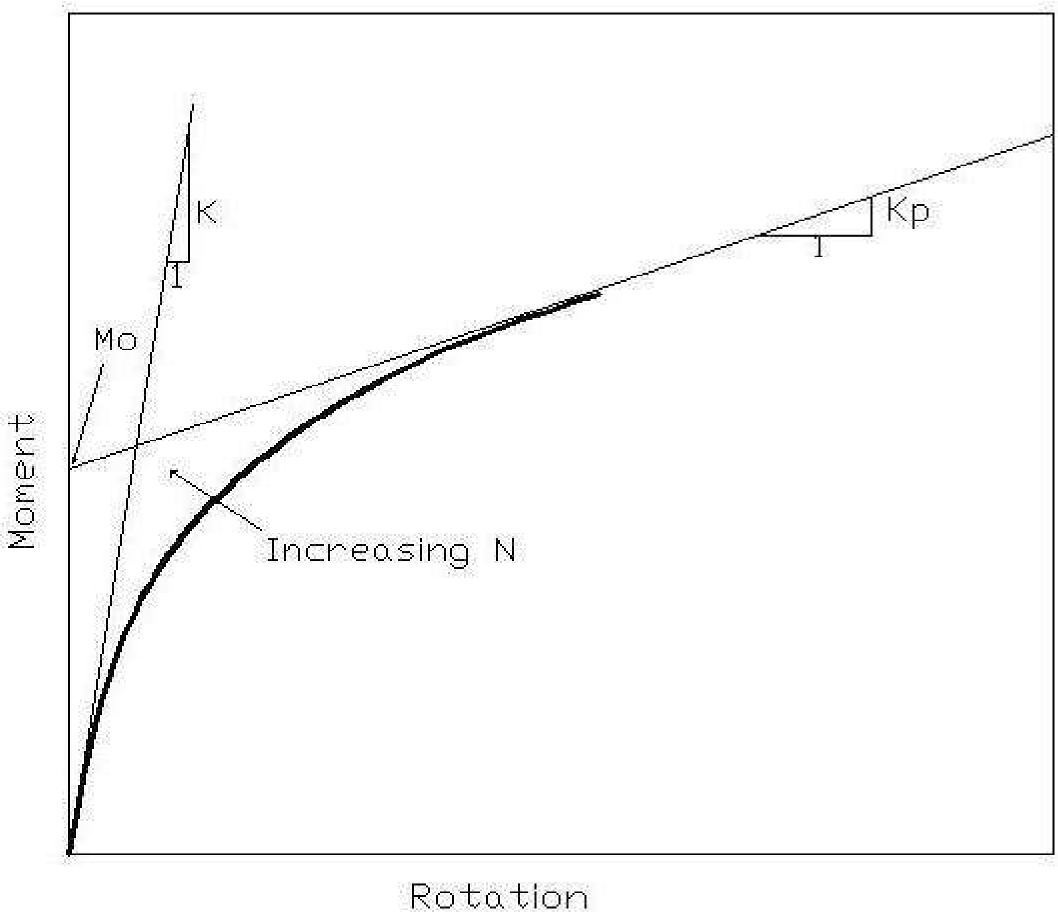

Fig. 2. Parameters of the Richard´s Model

If (M_b, θ_b) is the next reversal point, as shown in Fig. 3, the reloading relation between M and θ can be obtained by simply replacing (M_a, θ_a) with (M_b, θ_b) in Eq. (13). Thus, Eq. 10 is used if the connection is loading; if it is unloading or reloading, Eq. (13) should be used instead. The hysteretic damping produced during the loading, unloading and reloading process of the dissipater could be one of the most important sources of energy dissipation in the structure.

As stated earlier, the dissipater is modeled by a PR connection, which in turn is represented by the Richard´s Model. The friction forces developed at the upper and bottom brake lining pads of the dissipater (Fig. 1) times the depth of the beam will give the magnitude of the connection moment. The Richard Parameters are selected in such a way that force-displacement curves are approximated to those obtained from experimental results (small values of k_p, and large values of k and N). These parameters, and consequently their corresponding M-θ curves, change as the sizes of the beams change. For example, for Frame 3 (Fig. 4), there will be four different sizes of beams and dissipaters for this model.

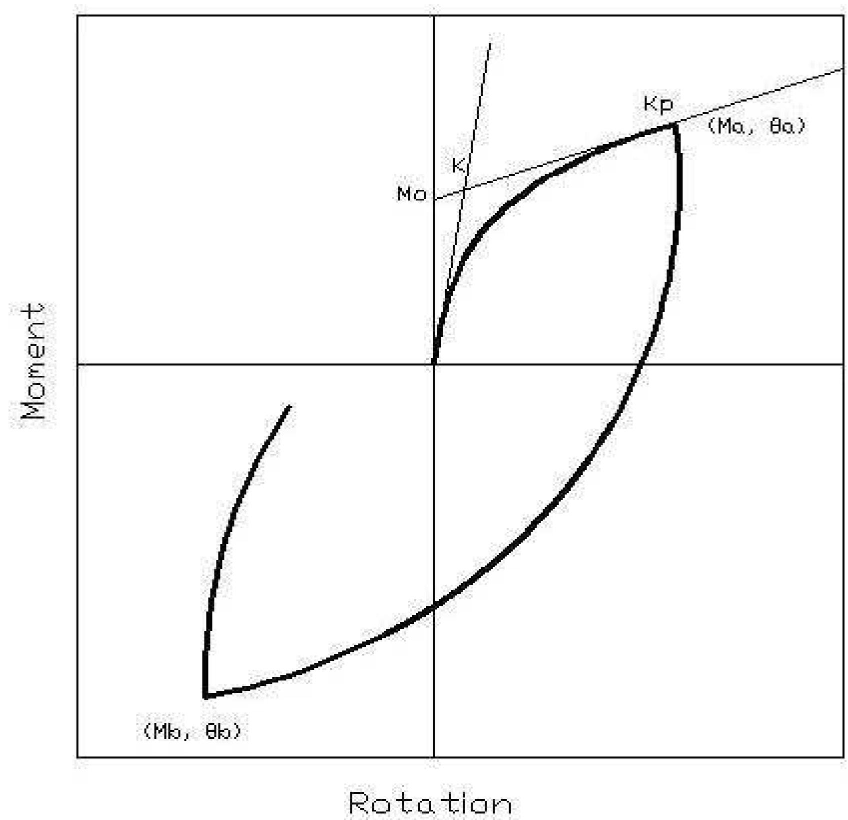

Fig. 3 Loading, unloading and reloading at the dissipaters

Structural and earthquakes models

Three steel moment resisting frame structures, representing different dynamic characteristics, are considered in the study. The frames are one, three, and eight stories. Their story height is a constant of 3.66 m and the span of each bay is 7.32 m. These frames were used for other researchers in analytical and experimental studies (Roeder et al 1993). Initially, the frames were designed according to UBC standards. Then, they were modified to generate three strong-column weak-beams (SCWB) models. Their geometry and member sizes are shown in Fig. 3. These frames are denoted hereafter as Frames 1 through 3. Their fundamental periods are 0.22, 0.49 and 1.07 sec., respectively. A critical damping of 2% (ξ=2%) is assumed in the frames. With the exception of exterior joints and the joints located on the top floor, the ratio of the sum of the plastic moments of the beams framing into a given beam-column joint to the sum of the plastic moments of the columns framing into the same joint, ranges from 0.76 to 0.96. All beams are made of A36 steel and the columns of Grade-50 steel, for all the models. These frames with different dynamic characteristics are subjected to twenty strong motion earthquakes representative of medium and stiff local soil conditions. They are referred hereafter as Earthquakes 1 through 20. The predominant periods of the earthquakes are given in Table 1. The used earthquakes are scaled down or up in such a way that the frames develop approximately a maximum interstory displacement of approximately 2%.

Results in terms of interstory displacements

The interstory displacements for Frame 1 are given in Table 2 for all the earthquakes. Four levels of the maximum friction force at the connection are considered. The corresponding maximum moments that can be developed (M_c) at the ends of the beams are *60%, 70%, 80%, and 90%* of the plastic moment (M_p). Thus the values of the ratio of M_c to M_p, denoted as *R*, are *0.6*, *0.7, 0.8 and 0.9*, respectively. *R=1.0* represents the frame without energy dissipaters. In this case, the maximum moment that can be developed is M_p. Results in the table indicate that the maximum interstory displacements can be significantly reduced when energy dissipaters are used. The displacements monotonically decrease as the *R* parameter decreases for most of the earthquakes. For a given value of the *R* parameter, no correlation is observed between the magnitude of the reduction and the predominant period of the earthquakes.

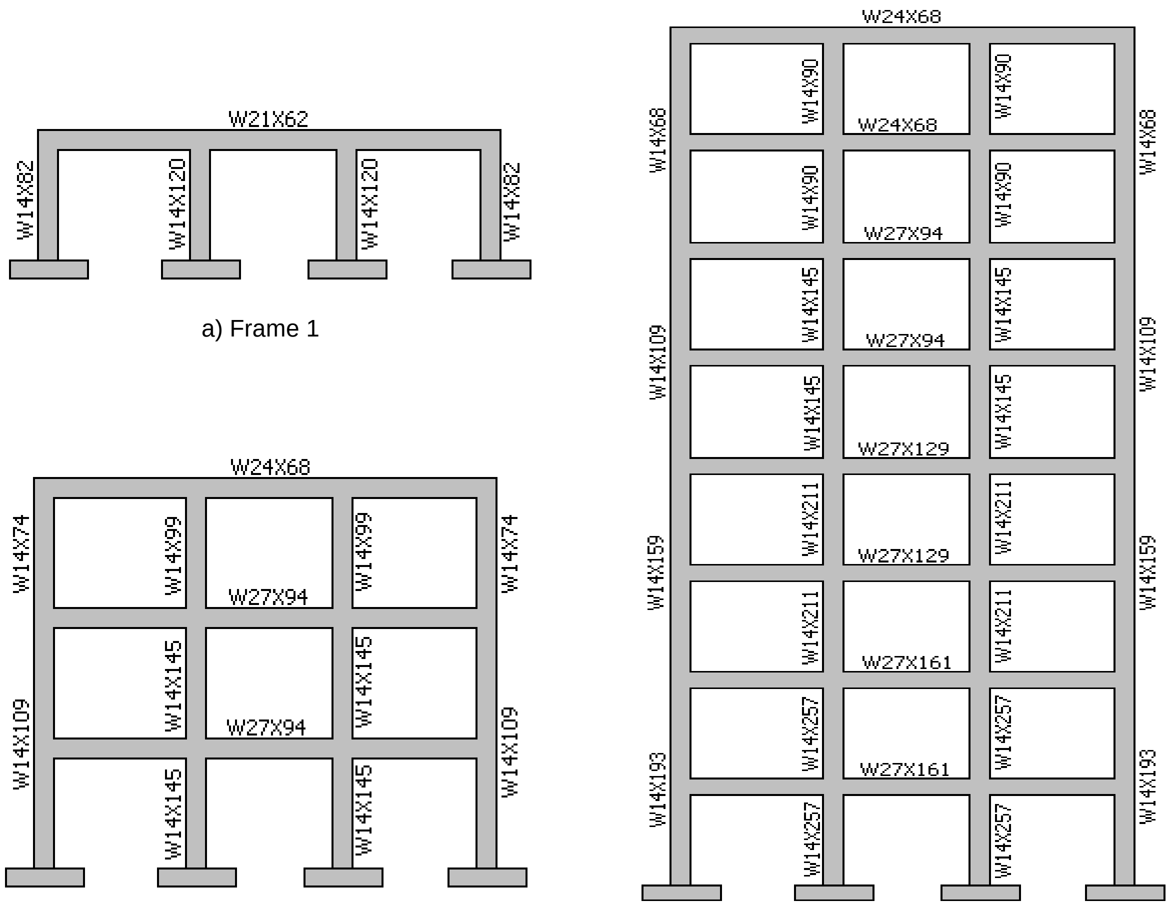

c) Frame 3

Fig. 4. Structural Models

Even though the stiffness of the frame with energy dissipaters is lower than that of the frame without dissipaters, the response under seismic loading largely depends on the dynamic characteristics of both the structure and the earthquake excitation. The frames with dissipaters may attract smaller inertial forces and at the same time dissipate more energy.

Representative results for Frame 2 are shown in Fig. 5 for a few earthquakes. As for the case of Frame 1, in some cases the interstory displacements decrease when energy dissipaters are used. However, unlike

Frame 1, no monotonic reduction of the displacements is observed as the *R* parameter decreases. In addition, the displacements of the frame with energy dissipaters are larger than that of the frame without dissipaters for some particular earthquakes and stories. It is also observed that, for a given value of *R*, the magnitude of the reduction significantly varies from one earthquake to another without show any correlation. Values of the displacements for Frame 3 were also estimated but are not shown since they don't give new information. From an observation of the results for all the frames and earthquakes it is concluded that the magnitude of the displacement reduction tends to decrease with the fundamental period of the frames. It is important to emphasize that, while many plastic hinges are formed in the frame without energy dissipaters, no plastic hinges are formed, in general, in the frames with dissipaters. Only one o two plastic hinges are formed in the frames with *R =0.9* for a few cases. It indicates that using energy dissipaters type friction protect the frames from significantly yielding**.**

Table 1. Earthquake models

EARTHQUAKE NUMBER	EARTHQUAKE NAME	STATION	PREDOMINANT PERIOD (Sec)
1	SAN FERNANDO	LAKE HUGHES ARRAY #12	0.17
2	SAN FERNANDO	PACOIMA DAM	0.21
3	NORTHRIDGE	LOS ANGELES WADSWORTH BLVD.	0.22
4	NORTHRIDGE	TOPANGA FIRE STATION	0.30
5	NORTHRIDGE	TOPANGA FIRE STATION	0.32
6	SAN FERNANDO	CASTAIC-OLD RIDGE ROUTE	0.34
7	SAN FERNANDO	CIT MILLIKAN LIB	0.35
8	NORTHRIDGE	LOS ANGELES, 1526 EDGEMONT AVE	0.39
9	SAN FERNANDO	450 N ROXBURY, BEVERLY HILLS	0.40
10	NORTHRIDGE	LOS ANGELES, WADSWORTH VA	0.48
11	NORTHRIDGE	LOS ANGELES, GRIFFITH OBSERVATORY	0.50
12	NORTHRIDGE	LOS ANGELES, 10660 WHILSIRE BLVD.	0.51
13	SAN FERNANDO	GRIFFITH PARK OBS	0.52
14	NORTHRIDGE	CANOGA PARK, SANTA SUSANA	0.57
15	NORTHRIDGE	HAWTHORNE FAA BLDG	0.60
16	EL CENTRO	ELC0	0.68
17	NORTHRIDGE	LOS ANGELES, 4929 WHILSIRE BLVD.	0.70
18	NORTHRIDGE	SHERMAN OAKS, 1525 VENTURA BLVD.	0.84
19	NORTHRIDGE	JENSON FILTRATION PLANT	1.15
20	NORTHRIDGE	LOS ANGELES, 4929 WHILSIRE BLVD.	1.21

Results in terms of interstory shears

The interstory shears for all the frames and the four levels of the friction force at the dissipater are also estimated. Results for Frame 1 are given in Table 2 and typical results for Frame 2 are given in Fig. 6. Some of the major observations made for the case of interstory displacements also apply to this parameter: a) the interstoy shears can be reduced by using energy dissipaters, and b) for a given value of

R and frame no correlation is observed between the magnitude of the reduction and the predominant period of the earthquakes. The only additional observations that can be made are that the reduction is more for interstory shears than for interstory displacements and that the relative reduction for interstory shears does not decrease with the fundamental period of the frames, as it does for the case of interstory displacements.

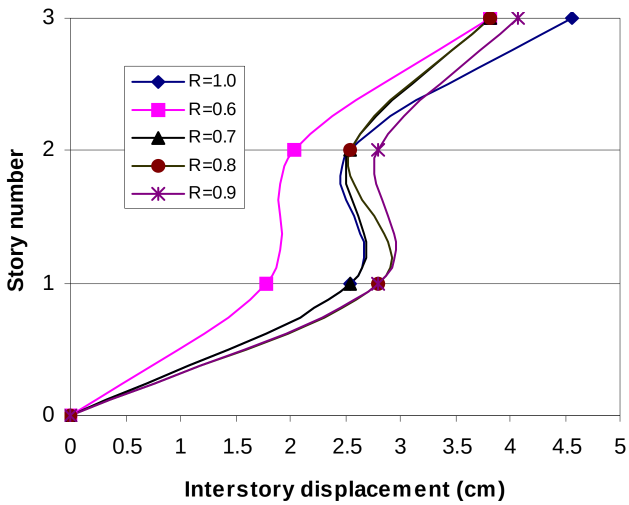

a) Earthquake 1

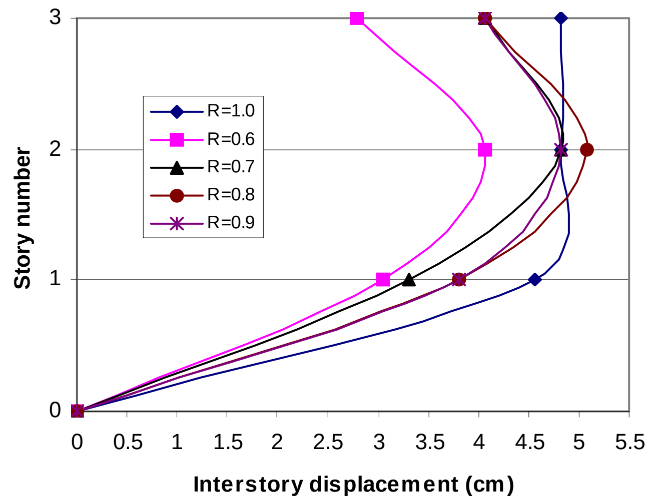

b) Earthquake 2

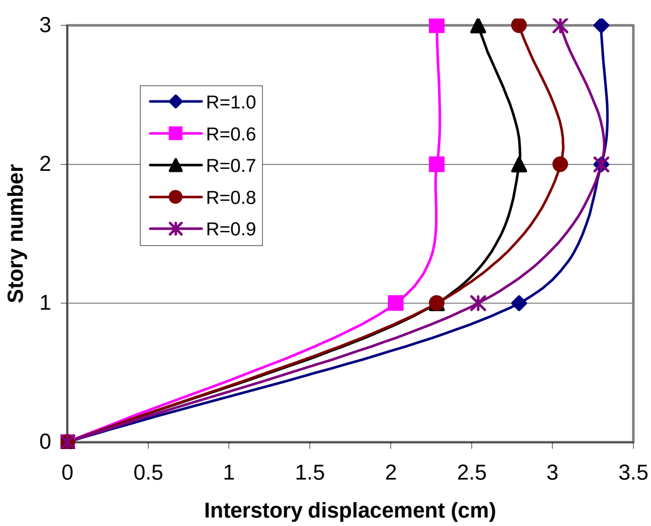

c) Earthquake 3

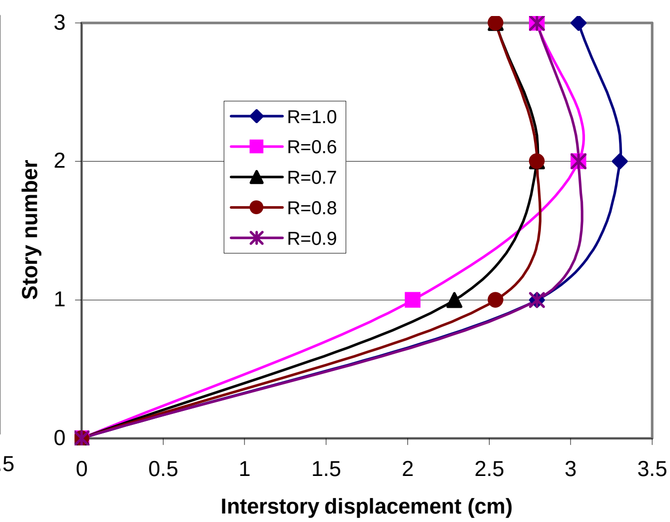

d) Earthquake 4

Fig. 5. Interstory displacements for Frame 2

Effectiveness of the dissipater in terms of equivalent viscous damping.

It has been shown that the use of energy dissipaters type friction can significantly reduce the maximum response of steel frames. In order to quantify the effectiveness of the dissipater, the reduction in terms of the total base shear is additionally studied. The amount of viscous damping (ξ_a) in the frame without energy dissipaters required to produce approximately the same reduction as that of the dissipater is estimated. The values of ξ_a for all the frames, *R* ratios and earthquakes used, are shown in Table 3. The results in the table clearly indicate that the equivalent viscous damping produced by energy dissipaters friction-type can be larger than that existing in a bare steel frame ($\xi \approx 2\%$). It is also observed that the ξ_a values increase as the *R* parameter decrease. In addition, no correlation is observed between the values of ξ_a and the predominant period of the earthquakes or the fundamental period of the frames.

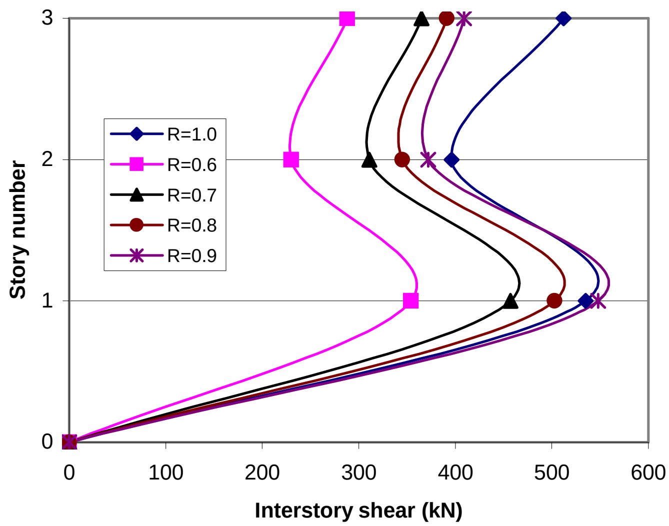

a) Earthquake 1

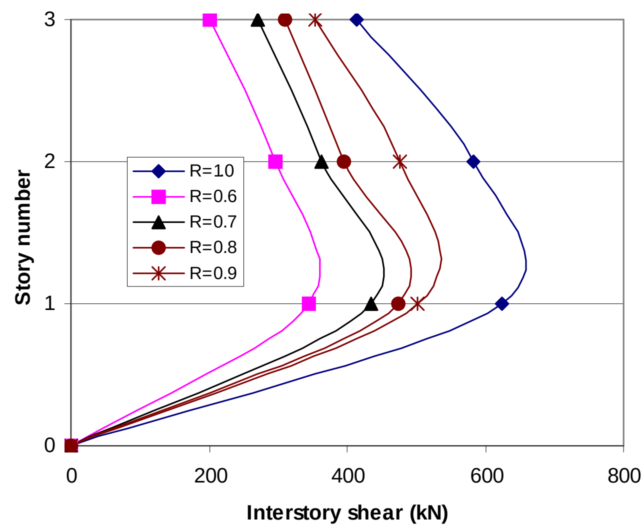

b) Earthquake 2

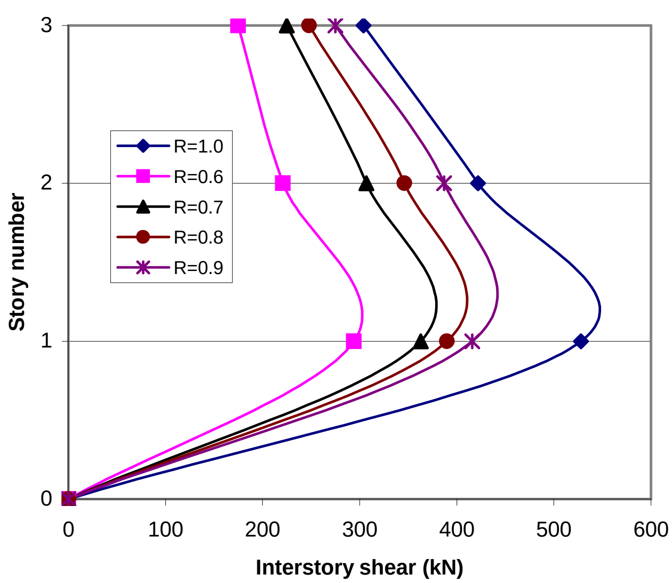

c) Earthquake 3

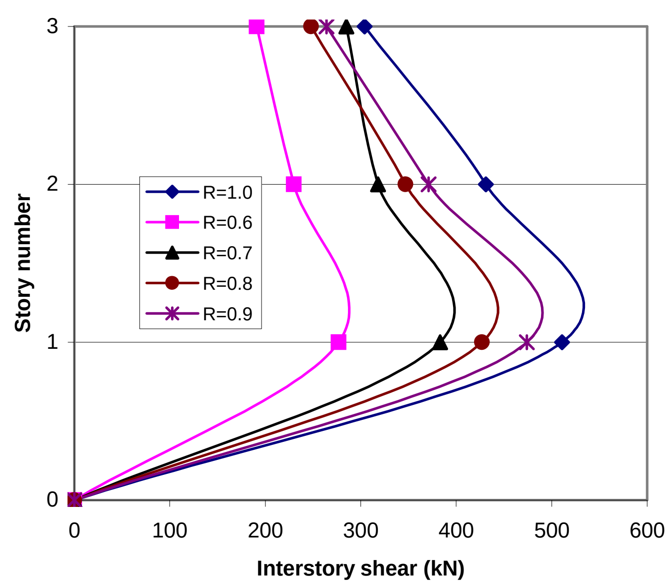

d) Earthquake 4

Fig. 6. Interstory shears for Frame 2

Table 2. Interstory displacements and shears for Frame 1

EARTHQUAKE NUMBER	INTERSTORY DISPLACEMENT (cm)					INTERSTORY SHEAR (kN)				
	R=0.6	R=0.7	R=0.8	R=0.9	R=1.0	R=0.6	R=0.7	R=0.8	R=0.9	R=1.0
1	2.00	2.60	2.66	2.68	2.81	238	358	371	375	395
2	2.45	2.90	3.11	3.13	2.88	277	377	412	422	404
3	2.34	2.40	2.43	2.43	3.04	251	324	338	339	421
4	2.33	2.94	3.27	3.59	5.01	251	358	396	422	538
5	2.31	2.50	3.05	3.22	2.86	248	343	385	416	401
6	2.73	3.12	2.69	2.63	3.81	285	356	361	365	498
7	2.97	3.37	3.47	3.40	3.77	279	372	407	432	479
8	3.23	2.88	2.96	2.96	3.34	265	352	378	401	439
9	1.84	2.55	2.78	2.85	2.81	229	328	368	393	394
10	3.21	3.36	3.12	3.22	4.25	330	389	420	428	537
11	2.70	2.72	2.91	3.24	3.06	266	349	385	417	422
12	2.82	3.21	3.09	3.15	3.93	301	375	387	416	448
13	3.10	2.83	2.99	3.08	3.53	307	360	399	418	454
14	4.77	4.52	4.75	4.76	3.82	377	447	473	476	480
15	3.05	3.15	3.09	3.20	3.26	275	365	404	418	498
16	3.00	2.99	2.88	2.95	3.11	296	359	387	408	436
17	3.85	3.61	3.53	3.51	3.95	337	398	430	438	509
18	3.67	3.58	3.35	3.36	3.44	313	378	412	425	488
19	2.06	1.87	1.86	1.86	2.88	233	260	260	260	254
20	5.10	4.42	4.16	4.01	4.27	417	440	460	460	496

Conclusions

The nonlinear seismic responses of moment resisting steel frames with energy dissipater devices (EDD) type friction are studied. The dissipaters are placed in the beam-column joint providing maximum flexibility for space utilization. Several moment resisting steel frames, representative of the short, medium and long period regions, and several strong motions, representative of medium and stiff local soil conditions, are used in the parametric study. In addition, the parameters of the device are modified to vary the magnitude of the friction force. Four levels of this parameter are considered. The values of the ratio of the corresponding maximum moments that can be developed (*Mc*) to the plastic moment (M_p), denoted as *R*, are *0.6, 0.7, 0.8* and *0.9*, respectively. *R*=1.0 represent the frames without dissipaters. The authors and their associates developed a finite element-based algorithm to evaluate the nonlinear seismic response of steel frames in time domain. The algorithm is able to model the seismic behavior of steel frames, including EDD and is used in the study. The numerical study indicates that EDD based on friction of metals can reduce the seismic response of steel frames in terms of interstory displacements and interstory shears. It is observed that the magnitude of the reduction for interstory displacements decreases with the fundamental period of the frames, but the reduction in terms of interstory shears is similar for all the frames. No correlation is observed between the reduction of either displacements or shears with the predominant period of the earthquakes. It is important to emphasize that, while many plastic hinges are formed in the frames without energy dissipaters, no plastic hinges are formed, in general, in the frames with dissipaters. Only one o two plastic hinges are formed in the frames with *R =0.9* for a few cases. It indicates that using energy dissipaters friction-type protect the frames from significantly yielding**.** In order to quantify the effectiveness of the dissipater, the required equivalent viscous damping to produce the same level of reduction of base shear as that of the dissipater, is estimated. It is clearly shown that the equivalent viscous damping of energy dissipaters friction-type can be much larger than that existing in a bare steel frame ($\xi \approx$ 2%). Based on this finding, design response spectra for MRSF with energy dissipaters friction-type can be developed for specific sites by using appropriate amounts of equivalent viscous damping.

Table 3. Equivalent viscous damping for the dissipaters

EARTHQUAKE NUMBER	R=0.6			R=0.7			R=0.8			R=0.9		
	M1	M2	M3	M1	M2	M3	M1	M2	M3	M1	M2	M3
1	3.2	6.5	2.2	0.5	1.5	0.8	0.4	0.1	0.4	0.3	0.1	0.3
2	3.0	6.0	9.5	0.3	3.9	0.3	0.2	2.3	2.5	0.2	1.3	1.5
3	5.2	5.5	2.7	2.0	3.0	0.4	1.8	2.2	0.3	1.6	1.8	0.5
4	5.0	5.0	2.1	1.5	2.1	1.6	0.7	1.3	1.9	0.6	0.5	1.2
5	3.0	5.0	4.2	0.6	2.1	2.5	0.2	1.2	1.5	0.2	0.5	0.3
6	3.1	10.0	7.0	1.3	4.7	6.5	1.3	3.7	5.2	1.3	2.5	3.0
7	4.2	8.3	5.0	1.5	5.5	2.0	0.8	3.5	1.6	0.5	2.5	0.7
8	3.3	3.5	10.0	1.2	0.5	4.4	0.8	0.5	6.0	0.5	0.5	7.1
9	4.9	10.0	6.0	1.5	2.3	1.4	0.6	1.1	0.6	0.1	1.0	0.2
10	7.0	8.0	4.5	3.1	5.1	0.8	2.1	3.3	0.8	0.5	2.0	0.7
11	4.5	4.8	7.0	1.4	2.1	1.2	0.6	1.4	0.8	0.4	0.8	0.5
12	4.4	2.8	10.7	1.3	0.6	5.8	0.8	0.1	2.2	0.3	0.3	0.4
13	6.5	9.0	4.5	0.3	3.2	3.0	1.5	2.0	2.0	1.2	1.4	0.1
14	6.0	10.0	4.0	5.5	4.3	1.8	3.5	2.5	0.6	1.2	1.4	0.3
15	7.9	4.5	5.5	1.0	7.3	3.3	0.4	5.5	2.5	0.1	2.0	1.5
16	10.0	12.0	6.0	4.5	6.5	1.9	3.0	3.2	1.1	0.3	2.0	0.9
17	9.0	8.0	9.0	5.0	11.0	2.9	2.5	8.0	1.7	1.5	8.0	0.7
18	6.0	10.0	1.5	1.9	3.8	1.5	1.5	2.2	1.0	1.0	1.5	0.7
19	3.0	8.0	10.5	1.1	3.6	5.4	0.4	2.5	4.0	0.0	2.0	0.4
20	4.3	11.0	1.9	3.0	3.0	0.6	1.6	1.9	0.1	1.1	1.5	0.3
MEAN	5.2	7.4	5.7	1.9	3.8	2.4	1.2	2.4	1.8	0.7	1.7	1.1

Keywords: energy dissipaters, seismic inelastic response, moment resisting steel frames, time history analysis, multi degree of freedom systems, friction of metals.

References

1. Applied Technology Council (1995). “Guidelines and Commentary for the Seismic Rehabilitation of Buildings”. *Report No. ATC-33-03*, Redwood City, CA.
2. Aiken, I.D., and Kelly, J.M. (1990), “Earthquake Simulator Testing and Analytical Studies of two Energy Absorbing Systems for Multistory Structures”, *Report No. UBC/EERC-90/03*, University of California, Berkeley.
3. Colson, A. (1991), “Theoretical Modeling of Semi-rigid Connections Behavior”, *Journal of Constructional Steel Research*, 19:213-224.
4. Filiatrault, A., and Cherry, S. (1997), “Performance Evaluation of Friction Damped Braced Steel Frames Under Simulated Earthquake Loads”, *Earthquake Spectra*, **3**(1), 57-78.
5. Gao, L., and Haldar, A. (1995), “Nonlinear Seismic Response of Space Structures with PR Connections”, *International Journal of Microcomputers in Civil Engineering*, 10, 27-37.
6. Grigorian, C.E., Yang, T.S., and Popov, E. (1993), “Slotted Bolted Connection Energy Dissipaters”, *Earthquake Spectra*, **9**(3), 491-504.
7. El-Salti, M.K., (1992), “Design of Frames with Partially Restrained Connections”, *PhD Tesis, Department of Civil Engineering and Engineering Mechanics, University of Arizona*.
8. Haldar, A., Nee, K.M. (1989), “Elasto-plastic Large Deformation Analysis of PR Steel Frames for LRFD”, *Computer & Structures*; **31**(5): 811-823.
9. Kullmann, H.G., and Cherry, S. (1996), “Full-scale testing of Concentrically Braced and Friction-Damped Braced Steel Frames Under Simulated Seismic Loading”, *Proceedings of the 11th World Conference on Earthquake Engineering, Acapulco, México*, Paper No. 958, Acapulco, México.
10. Kondoh, K., and Atluri S.N. (1987), “Large Deformation, Elasto-Platic Analysis of Frames Under Non-Conservative Loading, Using Explicitly Derived Tangent Stiffness Based on Assumed Stress”, *Computer Mechanics*, **2**(1), 1-25.
11. Pong, W.S., Tsai, C.S., and Lee G.C. (1994), “Seismic Study of Buildings Frames with Added Energy-Absorbing Devices”, *Technical Report NCEER-94-0016*, State University of New York at Buffalo.
12. Pall, A.S., Verganalakis V., and Marsh, C. (1987), “Response of Friction Damped Braced Frames”. *Journal of Structural Engineering Division, ASCE*, **108**(6), 1313-1323.
13. Pall, A.S. (1989), “Limited Slip Bolted Joints-A device to Control the Seismic Response of Large Panel Structures”, *PhD Thesis*, University of Montreal, Canada.
14. Reyes-Salazar, A. (1997), “Inelastic Seismic Response and Ductility Evaluation of Steel Frames with Fully, Partially Restrained and Composite Connections”, *PhD Thesis, Department of Civil Engineering and Engineering Mechanics, University of Arizona,* Tucson, AZ
15. Reyes-Salazar, A. and Haldar, A. (2000), “Dissipation of Energy in Steel Frames with PR Connections”, Structural *Engineering and Mechanics, An International Journal* 2000, **9**(3), 241-256.
16. Reyes-Salazar, A, Haldar, A. (2001), “Seismic Response and Energy Dissipation in Partially Restrained and Fully Restrained Steel Frames: An Analytical Study”, *Steel & Composite Structures, An International Journal*; **1**(4): 459-480.
17. Richard, R.M. (1993), “Moment-Rotation Curves for Partially Restrained Connections”, *PRCONN, RMR Design Group*, Tucson, Arizona.
18. Roeder, C.W., Scheiner, S.P., and Carpenter, J. (1993), “Seismic Behavior of Moment-Resisting Steel Frames: Analytical Study”, Journal *of Structural Engineering ASCE*, **119**(6), 1866-1884.
19. Shi, G., Atluri, S.N. (1988), “Elasto-plastic Large Deformation Analysis of Spaces-frames”, *International Journal of Numerical Method in Engineering*; **26**: 589-615.
20. Zhao, X.M., and Ha, K.H. (1996), “Friction Connections for Seismic Control of Moment Resisting Steel Frames”, *Proceedings of the 11th World Conference on Earthquake Engineering, Acapulco, México*, Paper No. 1963, Acapulco, México.